



ACCENTUATE FORTIFIED ARTIFICIAL INTELLIGENCE IN CONTROL TOPOLOGY FOR A DC-DC BOOST CONVERTER

Mr.R.GOPIKARAMANAN^{#1}, Mr.R.PRABURAJA^{#2}, Mr.S.SURESH.^{#3}

[#] Assistant Professor in Electrical and Electronics Engineering, Vel Tech university, Avadi, Chennai.

¹gopikaramanan@veltechuniv.edu.in, ²praburaja@veltechuniv.edu.in, ³ssuresh@veltechuniv.edu.in.

Abstract— In this manuscript a novel control topology of DC-DC boost converter using Model predictive control technique is used incorporated with kalman filter to determine about the variation in load a continuous and discrete time model of the converter for both voltage and current controller is modelled. The discrete switched mathematical model of the convert which serves as prediction model for MPC captures all operating mode of the Inductor current making it suitable for operation both in Continuous conduction mode(CCM) and Discontinuous conduction mode (DCM) hence the converter state can be predicted for the whole operating regime. For both MPC control schemes the converter switch is directly manipulated in order to meet the control objective. More over controller are augmented by load estimation scheme namely discrete time switched kalman filter is added to estimate converter states and to provide off free tracking of the output voltage due to tis integration action despite changes in the load in the way robustness of the controller is ensured when the converter operates under un nominal condition is simulated in this manuscript.

Keywords ----Boost converter, Model predictive control, Kalman filter, Continuous conduction mode, Discontinuous conduction mode etc...

I.INTRODUCTION

Over the past decade's dc-dc conversion has matured into ubiquitous technology, which is used in a wide variety of applications,including power supplies for computers, portable electronic devices, battery chargers,

and dc motor drives. In their simplest form dc-dc converters comprise two semiconductor switches that are periodically switched on and off, and a low-pass filter with an inductor and a capacitor. The filter is added to pass the dc component of the input and to remove the switching harmonics, and, thus, to produce at the output a dc voltage

With a small ripple. Usually, out of the two switches only one is controllable, the other is dually operated. However, more complex topologies have been introduced in the last years that use two bidirectional controllable switches. Despite the fact that the switch-mode dc-dc conversion is a well-established technology, the problems associated with these applications and their closed-loop controlled performance still pose theoretical and practical challenges. An appropriate control strategy should achieve the regulation of the output voltage of the converter to a desired value despite changes in the input voltage and the load, since such variations are very common; in many cases the input voltage is unregulated, e.g. when a rectifier and a dc-dc converter are connected in cascade, or the load is time-varying linear. DC-DC converters are intrinsically difficult to control due to their switching behavior, constituting a (Continuous time) switched linear or hybrid system. In particular depending on the position of the switches and the value of the current, there are three different operating modes, each one is governed by different linear continuous time dynamical laws. furthermore, the duty cycle is bounded between zero and one, while the current through the inductor cannot be



negative finally other constraints such as upper limit on the current during start up for a soft start, can be imposed based on the above, it is evident that a controller should turn on and off the controllable such that the output voltage becomes equal to its reference value. In general, this is achieved pulse width modulation technique. Hence by conforming the pulse width by modifying the duty cycle the output voltage is regulated to the desired level switch is directly manipulated i.e control signals are sent directly to the switch without the presence of an intermediate modulator. Regardless of the methodology employed with or without the presence of intermediate modulator. Regardless of the methodology employed with or without a modulator the control problem is to decide when the switch is to be turned on and off.

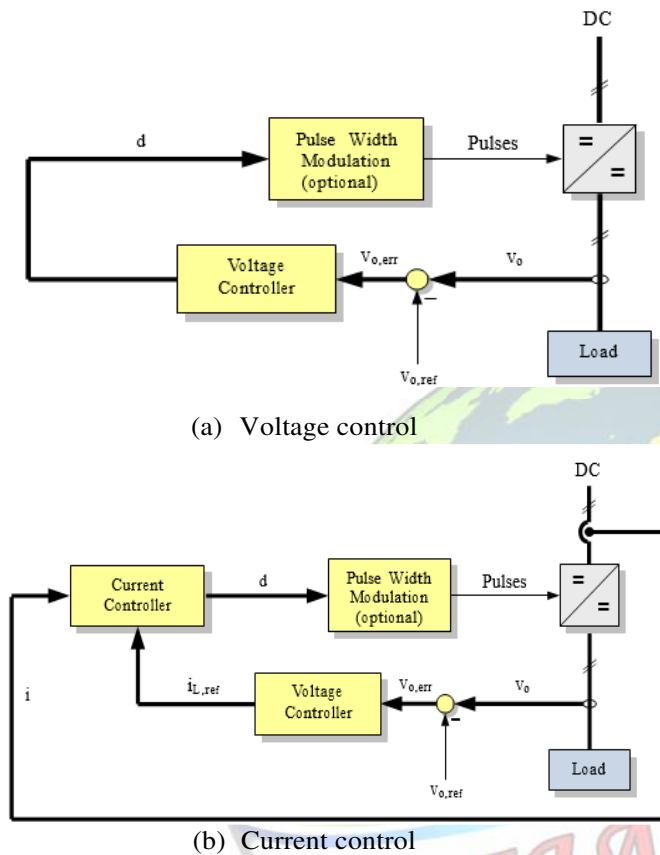
II. LITERATURE SURVEY

Many papers reported to literature with different control problems can be found in that they can be divided in to two main groups. They are Linear and Nonlinear controllers. Furthermore an additional classification would be based on the mathematical model of the converter used. The majority of the controller are based on the conventional PI controller. These schemes are tuned on the basis of the linear state space average model of the converter. The design procedure is trivial a crossover frequency is selected to be an order of magnitude smaller than 45degree and 60degree [1,8]. In [16,17] a linear quadratic regulator (LQR) is proposed. The controller is based on the locally linearized discrete time averaged model.in addition an outer estimation loop that effectively adds an integrator is employed. Nonetheless the limitations stem from the linear locally linearized while constraints cannot be handled. Throughout the years several nonlinear controllers are based on the averaged or non-averaged state space model of the converter have been proposed as well. Controllers based on fuzzy logic [12,19] and feed forward control [13,14] make use of the averaged model. However in these works the converter is considered lossless.in [21] the author design a family of PI controllers that depend nonlinearly on the control input i.e the Duty cycle. What is noteworthy in [80] is that nonlinear H(Infinity) controller is proposed the closed loop stability of

which is verified via Lyapunov function. In [18]a sliding mode controller as a current mode controller is designed. A sliding surface is output voltage is indirectly controlled. Furthermore stability and effects of controller parameter variations are investigated. Finally in [22]a detailed overview of sliding mode controllers for DC-DC converters is given while implementation related issues are addressed.

III. CONTROL OF DC-DC CONVERTERS

Many of the difficulties in controlling DC-DC converters arise from their hybrid nature. To bypass these obstacles, the modelling of the converter is based on state space averaging [8].with this modeling approach only the important dominant behavior of the plant is modeled, while other small but complicating phenomena are neglected. Therefore a mathematical of the converter is derived that uses the duty cycle as the system input. However duet approximations are made during the design process such as that the modulation frequency is much smaller that converter switching frequency, only the slow dynamics of the system are modeled only the basic insight is gained, since th switching nature of the system is ignored. Thereby with the averaging approach all information about the fast dynamics of the system is lost. The derived continuous time mathematical model is nonlinear since the state variables are multiplied with the duty cycle. In order to simplify the controller design procedure the nonlinear average model is linearized around a specific operating point. Nevertheless the linear controller are carried out with this procedure are usually tuned to achieve optimal performance only over a narrow operating range outside this range the performance is significantly deteriorated. For the closed loop operation of DC-DC converter several control techniques have been proposed, Which can be divided in to two main groups voltage mode and current mode controllers as shown in Fig 1[9]. In the first category the control objective is the elimination of the voltage error, i.e the difference between the measured output voltage and the reference value this is typically achieved by employing a single loop that directly controls the voltage as shown in fig 1 (a). The voltage control problem is difficult since it relates to a second order system with a non minimum phase behavior during transient [3]



(a) Voltage control

(b) Current control

Figure 1 General Block diagram of DC-DC Converter. In contrast to that current mode controllers employ two loops figure 1(b). The outer loop constitutes the voltage regulation loop, which manipulates the current reference so as to remove any output voltage error. The inner loop is the current regulation loop, which controls the measured or estimated inductor current along its reference. The switching state is typically manipulated indirectly via a modulator using the notion of the duty cycle. Despite the fact that for current mode controller two loops are required, this type of controller is more often employed since the design procedure is simpler, the current exhibits a minimum phase behavior with respect to the control action (and it is first order system). Model predictive controller (MPC) has been typically used in its simplest form namely as a dead beat controller for controlling the predominant DC-DC converter topologies, i.e. the buck, the boost and buck

boost converter [4,5,6,20,22]. A more complex MPC strategy was introduced in [10,11] for the buck and in [2,3] for boost converter. In this work, MPC strategy was introduced in [10,11] for the buck and in [2,3] for the boost converter. In this work MPC is employed as both a current and voltage mode controller. A discrete time model of the converter is introduced which captures all operating modes of the inductor current making it suitable for operation both in continuous conduction mode (CCM) and discontinuous conduction mode (DCM) for both MPC based schemes. Enumeration is used, i.e. all the possible switching (current or voltage controller) different strategies to tackle the inherent increased computational complexity are presented. Furthermore, a state estimation scheme is implemented that addresses load uncertainties and model mismatches.

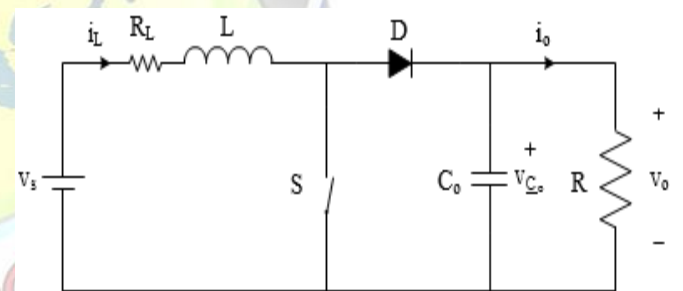


Figure 2 Topology of DC-DC boost converter

IV MODEL OF THE BOOST CONVERTER

A. Continuous Time Model

The converter can operate in continuous (CCM) and discontinuous (DCM) depending on the value of the inductor current $i_L(t)$ as shown in figure 3. Three different linear dynamics are associated with the switch positions that capture all operating modes of the inductor current. When the switch S is on ($S=1$), energy is stored in the inductor L and the inductor current $i_L(t)$ increases. When the switch S is off ($S=0$), the inductor is connected to the output and energy is released through it to the load, resulting in decreasing $i_L(t)$. Furthermore, when the switch S remains off and $i_L(t)=0$, then both S and D are off, and the topology is reduced to the mesh formed by the capacitor C_0 and the load. In the case the converter operates in DCM.

The state space representation of the converter in the continuous time domain is given by the following equation [9].

$$\frac{dx(t)}{dt} = (A_1 + A_2 u(t) + B v_s(t))$$

$$y(t) = Cx(t)$$

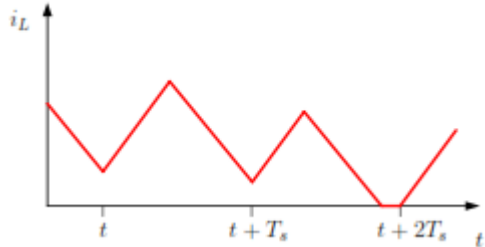


Figure 3 The shape of the inductor current reveals the operation mode of the converter operates CCM from t to T_s and in DCM from $t+T_s$ to $t+2T_s$.

2. The inductor current is positive and the switch is off for the whole sampling interval i.e $i_r(k) > 0$ $i_L(k+1) > 0$ and $S=0$.
3. During the sampling interval the inductor current reaches zero while the switch is off i.e $i_r(k) > 0$ $i_L(k+1) > 0$ and $S=0$.
4. The inductor current is zero and the switch is off for the whole sampling interval i.e $i_L(k) = i_L(k+1) = 0$ and $S=0$

$$x(k+1) = \begin{cases} E_1 x(k) + F_1 v_1(k) & \text{Mode 1} \\ E_2 x(k) + F_2 v_2(k) & \text{Mode 2} \\ E_3 x(k) + F_3 v_3(k) & \text{Mode 3} \\ E_4 x(k) & \text{Mode 4} \end{cases} \quad (2)$$

$$y(k) = Gx(k) \dots (2)$$

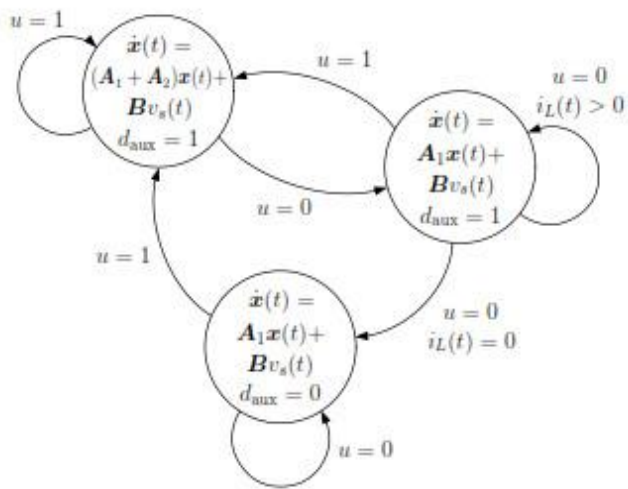


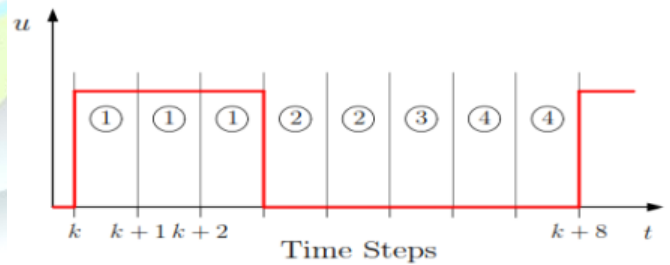
Figure 4 DC-DC converter presented as a Continuous time automation.

The derivation of the adequate model of the boost converter to serve as an internal prediction model for MPC is of fundamental importance. As can be seen in figure after discretization of the model in time the converter can operate in four different mode depending on the shape of the inductor current.

1. The inductor current is positive and the switch is on for the whole sampling interval i.e $i_r(k) > 0$ $i_L(k+1) > 0$ and $S=1$.



(a) Inductor current



(b) Switch position

Figure 5 operational model used in mathematical model to describe converter

B. OPTIMAL CONTROL OF DC-DC BOOST CONVERTER

The following two different MPC approaches to the control problem will be presented. In the first approach the control problem is tackled as a current regulation problem while in the second as a voltage regulation.

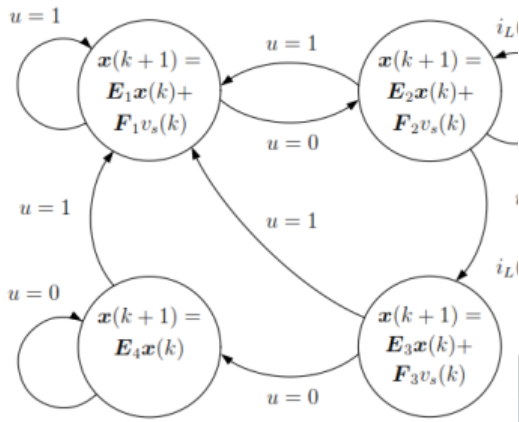
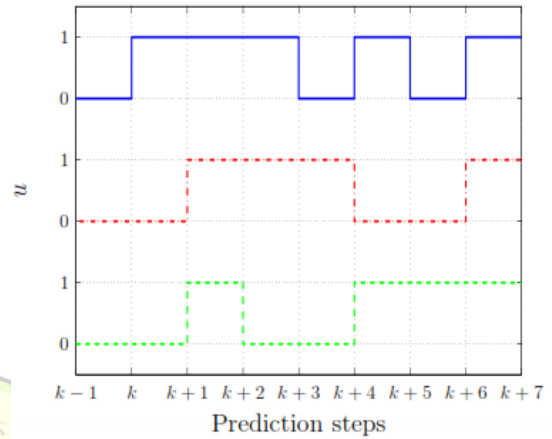


Figure 6 Discrete time mathematical model of the DC-DC Converter represented as a Discrete time automaton



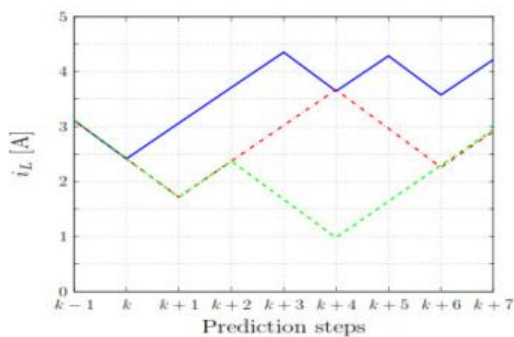
(b) Predicted switch sequence
Figure 6 Three candidate switching sequence for prediction horizon N=7

C. DIRECT MODEL PREDICTIVE CURRENT CONTROL

The introduced MPC approach indirectly control the output voltage by controlling the inductor current see Figure 1(b). This is achieved by approximately manipulating the controllable switch to derive the optimal sequence of control actions that minimizes a user defined objective function subject to the plant dynamics, an enumeration techniques is used. Since in the control method introduced here the control problem is formulated as a current regulation problem, the deviation of the inductor current from its reference defined as

$$i_{L, err}(K) = i_{L, ref} - i_L(K) \dots \dots (3)$$

In order to precisely describe the control problem two different objective functions are proposed. In the first approach the average value of the current error is penalized, while in the second rms value of the current error is considered. This allows us to use a shorter prediction horizon.



(a) Prediction current strategy

In the following two alternatives formulations of the objective function are described

D. Average current error

At time steps k, the average current error over the prediction interval NTs is given by

$$i_{L, err, avg}(k) = \frac{1}{NTs} \int_{kTs}^{(k+N)Ts} |i_{L, err} \left(\frac{t}{k} \right)| dt \dots (4)$$

The above integral can be rewritten as

$$i_{L, err, avg}(k) = \frac{1}{N} \sum_{l=k}^{k+N-1} |i_{L, err} \left(\frac{l}{k} \right)| \text{ with}$$

$$i_{L, err} \left(\frac{l}{k} \right) = \frac{i_{L, err} \frac{l}{k} + i_{L, err} \left(l + \frac{1}{k} \right)}{2}$$

Based on the above equation the objective function is

$$J_{avg}(K) = \sum_{t=k}^{k+N-1} \frac{1}{N} |i_{L, err} \left(\frac{l}{k} \right)| + \lambda \left| \Delta u \left(\frac{l}{k} \right) \right| \dots (5)$$

The second term in the above equation penalizes the difference between two consecutive switching states

$$\Delta u(k) = u(k) - u(k-1)$$

The term is added to decrease the switching frequency and to avoid excessive switching. The weighting factor $\lambda > 0$ sets the tradeoff between the inductor current error and the switching frequency. In [31] some guide lines for tuning the weighting factor are given. Further more it should be noted that the switching frequency varies depending on the operating point of the converter. The sampling interval T_s serves as an upper bound on the switching frequency i.e $f_{sw} \leq (1/2T_s)$ regardless of the operating point the switching frequency cannot be higher than half the sampling frequency. The equality corresponds to the case when $\lambda=0$ the output voltage is twice the input voltage i.e $V_o=2V_s$ and when the inductor is ideal with $R_L=0$.

E. RMS current error

The rms value of the current error over the prediction intervals is equal to

$$i_{L, err, rms}(k) = \frac{1}{NT_s} \sqrt{\int_{kTs}^{(k+N)Ts} |i_{L, err}\left(\frac{t}{k}\right)| dt} \dots (6)$$

With the current error given in the above expression is equivalent to

$$i_{L, err, rms}(k) = \frac{2}{3N} \sum_{l=k}^{k+N-1} \left| 2\bar{i}_{L, err}\left(\frac{l}{k}\right) - \bar{i}_{L, err}\left(\frac{l}{k}\right) \right| \text{ where}$$

$$\bar{i}_{L, err}\left(\frac{l}{k}\right) = \frac{i_{L, err}\left(\frac{l}{k}\right) + i_{L, err}\left(\frac{l+1}{k}\right)}{2}$$

The objective function of the rms current error based on this approach is given by

$$J_{rms}(K) = \sum_{l=k}^{k+N-1} \frac{2}{3N} \left| 2\bar{i}_{L, err}\left(\frac{l}{k}\right) - \bar{i}_{L, err}\left(\frac{l}{k}\right) \right| + \lambda \left| \Delta u\left(\frac{l}{k}\right) \right| \dots (7)$$

Load variation

The kalman filer estimates the converter states and provides offset- free tracking of the output voltage due to its integrating action despite, changes in the load. In that way the robustness of the controller is ensured even when the converter operates under nonnominal conditions. Therefore this additional loops is

employed to provide state estimates to the previously derived optimal controller where the load was assumed to be known and constant. The output voltage reference will be adjusted so as to compensate for the deviation of the output from its actual reference.

Block diagram of the Model predictive control scheme with Kalman filter to estimate the load variation is shown in the below figure.

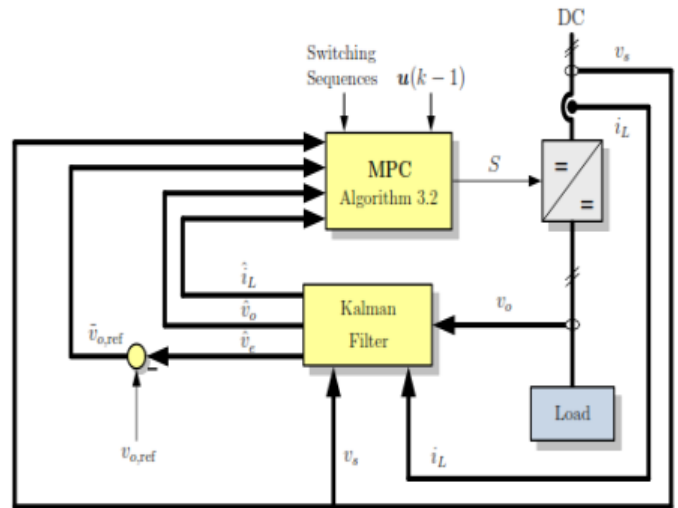


Figure 7 Block diagram of the MPC with voltage control scheme and Kalman filter

V. ALGORITHMS AND FLOW CHART OF CONTROL STRATEGY

A. Algorithm for Direct current mode MPC

```

function  $\mathbf{u}^*(k) = \text{CURRMPC}(\hat{\mathbf{x}}(k), \mathbf{u}(k - 1))$ 
 $J_{\dagger}^*(k) = \infty; \mathbf{u}^*(k) = \emptyset; \mathbf{x}(k) = \hat{\mathbf{x}}(k)$ 
for all  $\mathbf{U}$  over  $N$  do
     $J_{\dagger} = 0$ 
    for  $\ell = k$  to  $k + N - 1$  do
         $\mathbf{x}(\ell + 1) = f_{\dagger}(\mathbf{x}(\ell), \mathbf{u}(\ell))$ 
         $i_{L, \text{err}, \dagger}(\ell) = g_{\dagger}(\mathbf{x}(\ell), \mathbf{x}(\ell + 1))$ 
         $\Delta \mathbf{u}(\ell) = \mathbf{u}(\ell) - \mathbf{u}(\ell - 1)$ 
         $J_{\dagger} = J_{\dagger} + i_{L, \text{err}, \dagger}(\ell) + \lambda |\Delta \mathbf{u}(\ell)|^p$ 
    end for
    if  $J_{\dagger} < J_{\dagger}^*(k)$  then
         $J_{\dagger}^*(k) = J_{\dagger}, \mathbf{u}^*(k) = \mathbf{U}(1)$ 
    end if
end for
end function

```

Algorithm for Direct current mode Model predictive control method is shown in above pseudo code, to achieve the desired control on dc-dc boost converter a real time optimization problem is framed and solving the problem with constraints in real time using enumeration technique the user defined objective function is minimized subjected to converter dynamics.

Algorithm for Direct voltage control mode MPC

```

function  $\mathbf{u}^*(k) = \text{VOLT MPC}(\hat{\mathbf{x}}(k), \mathbf{u}(k - 1))$ 
 $J^*(k) = \infty; \mathbf{u}^*(k) = \emptyset; \mathbf{x}(k) = \hat{\mathbf{x}}(k)$ 
for all  $\mathbf{U}$  over  $N$  do
     $J = 0$ 
    for  $\ell = k$  to  $k + N - 1$  do
        if  $\ell < k + N_1$  then
             $\mathbf{x}(\ell + 1) = f_1(\mathbf{x}(\ell), \mathbf{u}(\ell))$ 
        else
             $\mathbf{x}(\ell + 1) = f_2(\mathbf{x}(\ell), \mathbf{u}(\ell))$ 
        end if
         $v_{o, \text{err}}(\ell + 1) = \bar{v}_{o, \text{ref}} - v_o(\ell + 1)$ 
         $\Delta \mathbf{u}(\ell) = \mathbf{u}(\ell) - \mathbf{u}(\ell - 1)$ 
         $J = J + |v_{o, \text{err}}(\ell + 1)| + \lambda |\Delta \mathbf{u}(\ell)|$ 
    end for
    if  $J < J^*(k)$  then
         $J^*(k) = J, \mathbf{u}^*(k) = \mathbf{U}(1)$ 
    end if
end for
end function

```

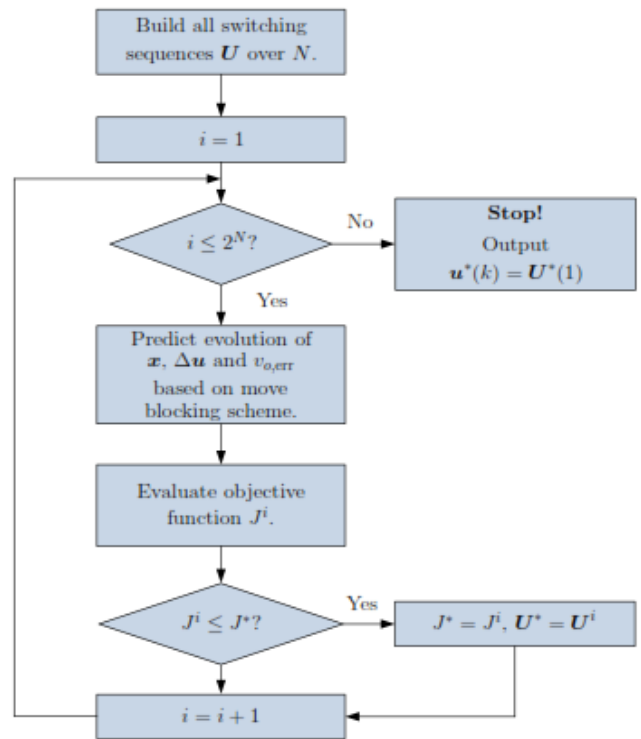


Fig 9 Flowchart for Direct MPC Voltage control algorithm.

VI SIMULATION RESULT AND DISCUSSION

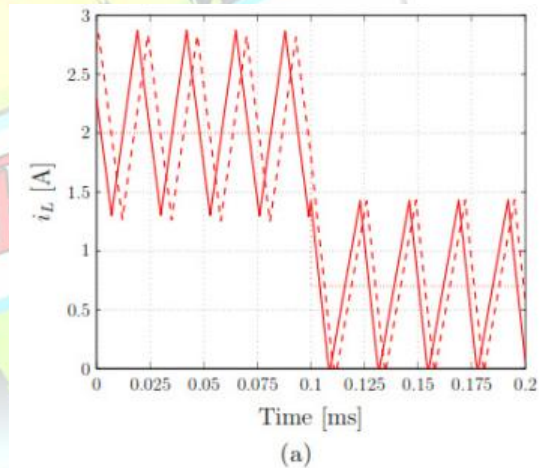
A. CURRENT MODE MPC

The simulations focus on the new MPC strategy for the current loop and its dynamical properties at this point the behavior of the whole system is not presented is not presented to not obstruct the dynamical analysis . Thus for both approaches the same scenario is examined namely a step down change in the inductor current reference. The behavior of the converter in both CCM and DCM is examined. The circuit parameters are $L=150\mu\text{H}$, $R_L = 0.2\Omega$ and $C_O = 220\mu\text{F}$. The load resistance is assumed to be known and constant for all operating points it is equal to $R=73\Omega$. Initially the input voltage is set equal to $V_s=20\text{V}$, while the output reference voltage is set equal to $v_{o,ref}=53.5$ Corresponding to the reference inductor current $i_{L,ref} = 2\text{A}$. Regarding the objective function the weighting factor is tuned in such a way that the switching frequency in both approaches is approximately the same i.e $\lambda=0.3$ for the first approach and $\lambda=0.6$ for the second. The prediction horizon is $N=5$ and the sampling interval is $T_s=2.5 \mu\text{s}$. The converter initially operates under nominal conditions. At time $t=0.1\text{ms}$ a change to the inductor current reference from $i_{L,ref}=2\text{A}$ to $i_{L,ref}=0.7\text{A}$ occurs. As can be seen in the figure 10 for both the approaches the inductor current reaches very quickly the new desired level. The switching frequency is about $f_{sw}= 45 \text{ kHz}$. Since the operating points and the corresponding are the same in both the approaches can be observed in Figure 11, which relates to the converter operating under nominal and steady state conditions. The impact of varying weighting factor λ is investigated. The corresponding output voltage error, given by

$$v_o = \sqrt{\left(\frac{1}{N} \left(\sum_{k=1}^N v_{o,ref} - v_o(k)\right)^2\right)} \dots (8)$$

The switching frequency f_{sw} . As depicted. As can be seen the average error current based approach results in a lower switching frequency with zero tracking error which means that lower switching losses can be achieved with this approach. On the other hand the rms current error based approach leads to higher switching frequencies when λ is

very small due to the quadratic penalty such high switching frequencies tend to result in even faster transient responses. This can be shown in figure 13 and 14. When the weighting factor is tuned to be the same in both approaches i.e $\lambda = 0.3$ then the dynamical behavior of the system differs in the fig 13 the response of the controller in a step up change in the current referee is depicted. At time $t=0.1 \text{ rms}$ a change to the inductor current reference from $i_{L,ref}=2\text{A}$ to $i_{L,ref}=3\text{A}$ occurs. As can be seen in fig 13 the inductor current very quickly reaches the new desired level in both approaches. However as mentioned above, Due to the quadratic penalty used in the second approach (rms-based approach) the deviation of the current from its reference is penalized more heavily resulting in a smaller ripple, thus in a higher switching frequency. Because of these reasons further more a step down variation in the current reference slightly faster furthermore a step down variation in the current reference is investigated. At time $t=0.1\text{ms}$ the reference value changes from $i_{L,ref} = 3\text{A}$ to $i_{L,ref} = 1\text{A}$. The response of the converter depicted in the figure 14.



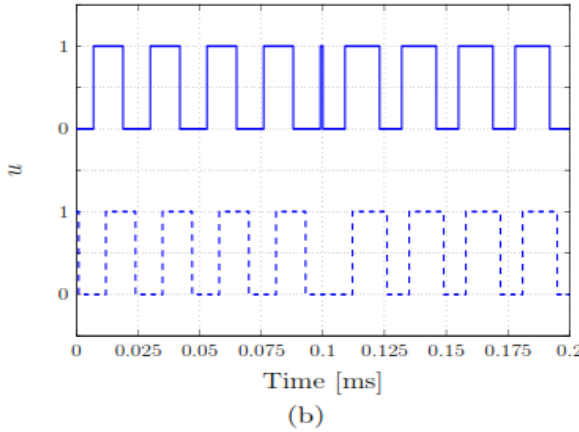
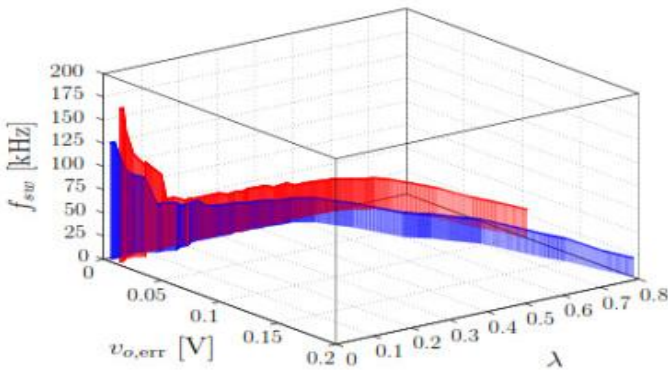


Figure 11 Simulation result for step down change scenario.

- (a) Inductor current for the first (solid line) and the second (dashed line) approach. Inductor current reference (dotted line).
- (b) Pulse for the first (solid line) and second (dashed line) approach.

In both the approaches the current decreases very fast its new desired level the behavior of the controller for both approaches is very similar and the same observations are made i.e the current in the second approach settles to its reference faster. Finally as can be seen for the average based approach, because of the high ripple current the converter operates in DCM since the current reaches zero for an amount of time.

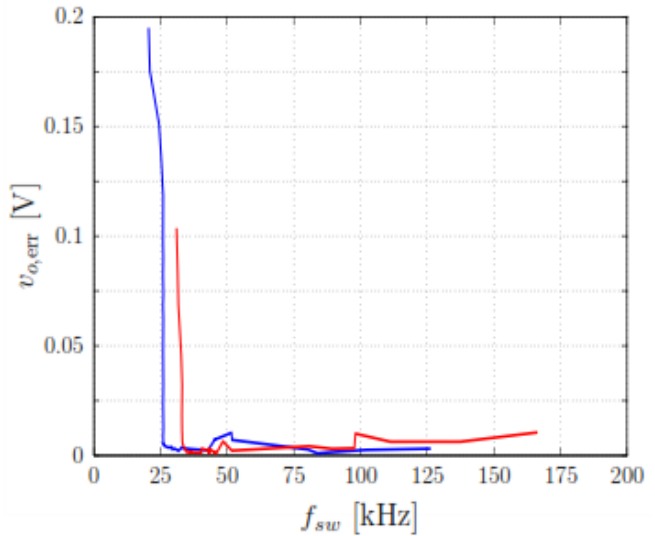


- (a) The output voltage error $v_{o,err}$ and corresponding switching frequency f_{sw} versus the weighting factor λ .
- (b) The voltage error $v_{o,err}$ versus switching frequency f_{sw} .

Figure 12 Effect of weighting factor λ on the output voltage error and the switching frequency f_{sw} for the average current error based (blue) and the rms current error based (red) approaches the converter operates under nominal condition.

B. VOLTAGE MODE MPC

In this section simulation results are presented to demonstrate the performance of the proposed voltage mode controller under several operating conditions. Specifically the closed loop converter behavior is examined in both CCM and DCM. The dynamic performance is investigated during startup moreover the response of the output voltage to step changes in the commanded voltage reference the input

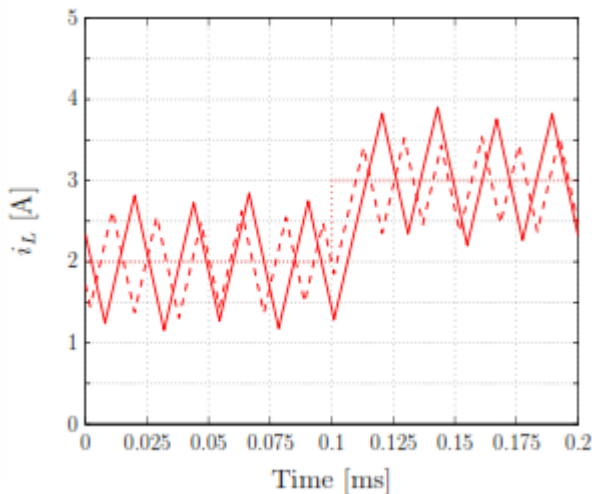


voltage and the load are illustrated. The circuit parameters are $L=450\mu\text{H}$, $R_L=0.3\Omega$ and $C_o=220\mu\text{F}$. The nominal load resistance is $R=73\Omega$ if not otherwise started the input voltage is $V_s=10\text{V}$ and the reference the input voltage is $V_{o,ref}=15\text{V}$. the weight in objective function is $\lambda=0.1$ the prediction horizon is $N=14$ and the sampling interval is $T_s=2.5\mu\text{s}$. A moving block scheme is used with $N_1=8$, $N_2=6$ and $n_s=4$ i.e the sampling interval for each of the last six steps in the prediction interval is

$T_s=10\mu s$ note that the length of the prediction horizon in time should be as long as possible. A horizon of about $80\mu s$ is sufficient. The first part of the prediction horizon should be finely sampled since switching is possible only at the sampling instants. As such the sampling interval T_s should be as small as possible. The number of steps in the prediction horizon $N=N_1+N_2$ determines the computational complexity. To ensure that the control law can be computed within T_s , N should be relatively small leading to the choice made above final the covariance matrices of the kalman filter are chosen.

(b)Pulses for the first (solid line) and the second (dashed line) approach.

Figure 13 Simulation result for step down scenario



(a) Inductor current for the first (solid line) and second (dashed line) approach and inductor current reference (dotted line)

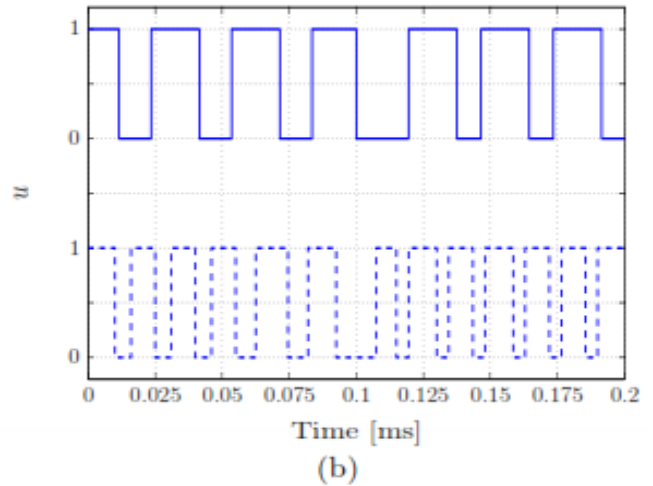
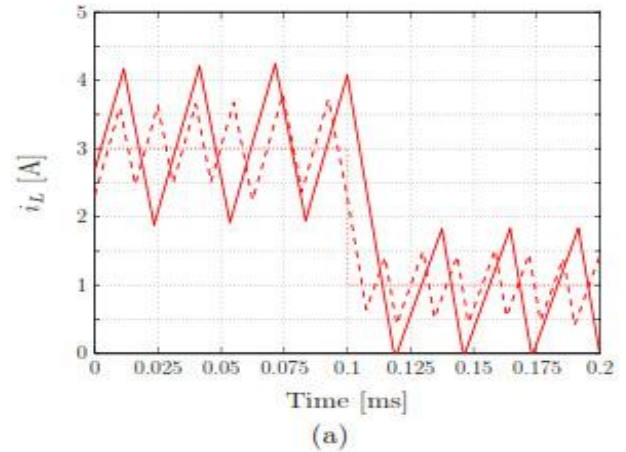
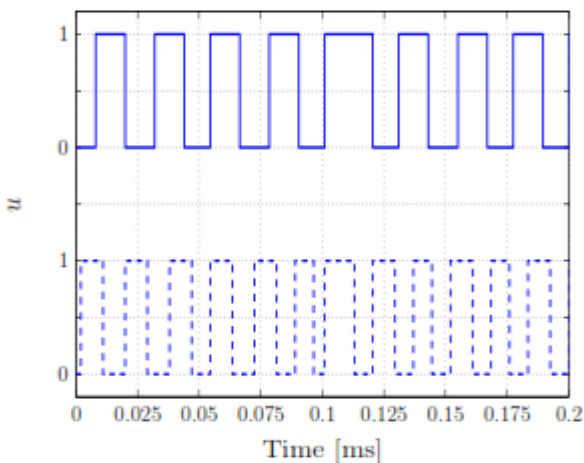
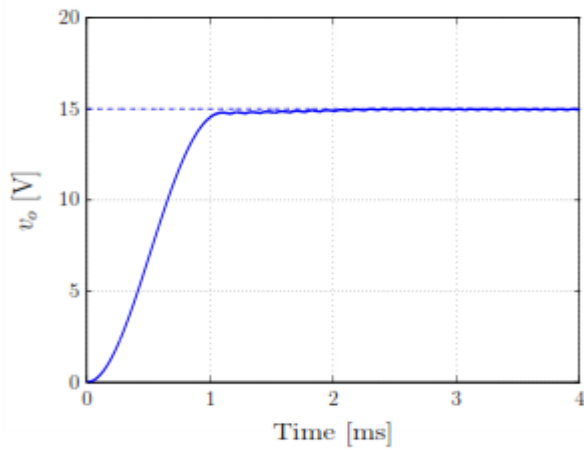


Figure 14 simulation results for step down scenario

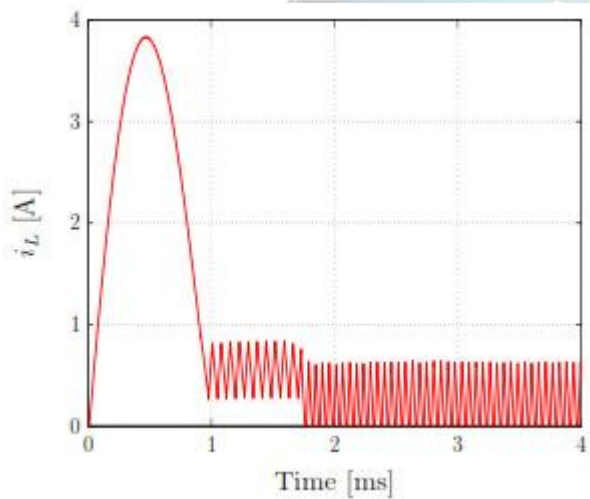
C.NOMINAL START UP

The first case to be examined is that of the startup behavior under nominal conditions. As can be seen in figure 15 the inductor current is very quickly increased until the capacitor is charged to the desired voltage level. The output reaches its desired value in about $t=1.8ms$ without any noticeable overshoot. Subsequently, the converter operates in DCM with the inductor current reaching zero.





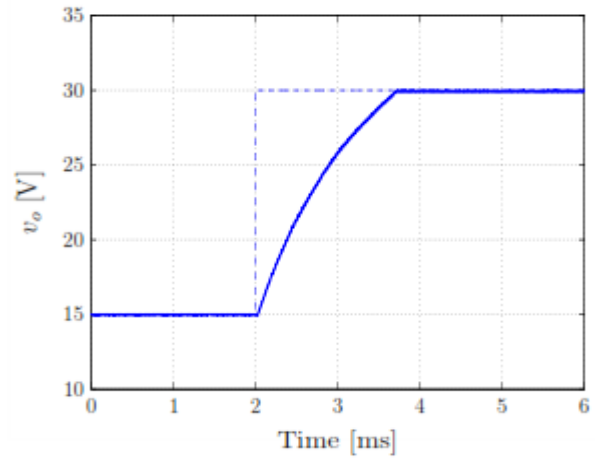
(a) Output voltage (solid line)and output voltage reference dashed line



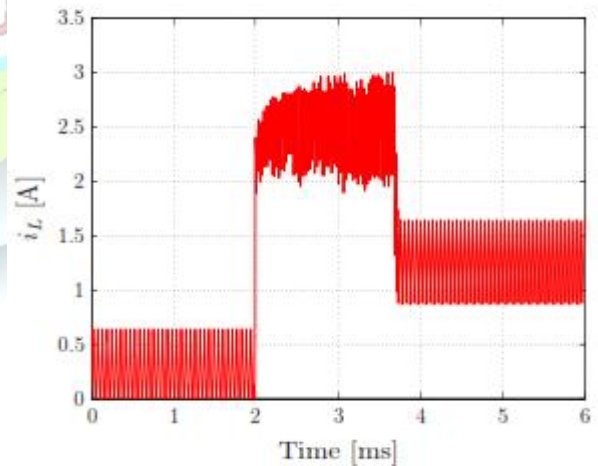
(b) Inductor current

Figure 15 simulation result for Nominal start up

controller increase the current temporarily in order to quick ramp up the output voltage. Note that this favorable choice is made by the controller thanks to its long prediction horizon and despite the non-minimum phase behavior of the converter. Once the output voltage has reached its reference, the inductor current is decreased to the level that corresponds to the steady state power balance. The controller exhibits an excellent behavior during the transient reaching the new output voltage in about $t=1.8\text{ms}$ without any overshoot.



(a) Output voltage (solid line) reference (dashed line)



(b) Inductor current

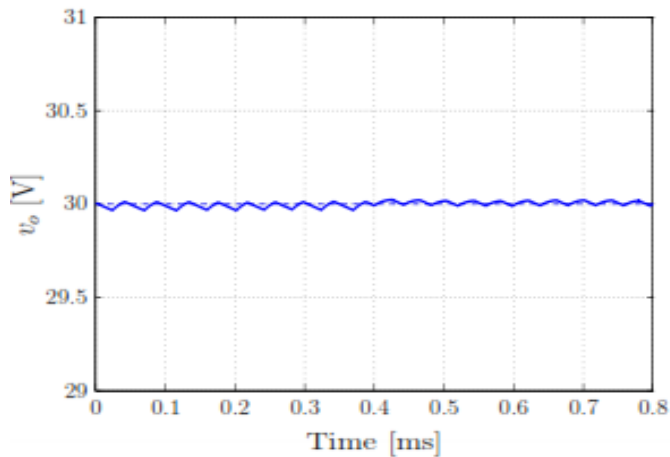
Figure 16 simulation result for step down change

D.STEP CHANGES IN THE OUTPUT REFERENCE VOLTAGE

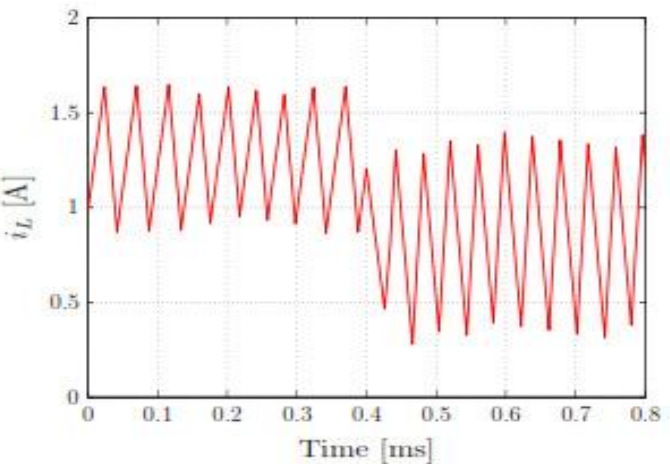
First step up change in the output reference voltage is examined at time $t=2\text{ms}$ the reference is doubled from $V_{0\text{ref}}=15\text{V}$ to $V_{0\text{ref}}=30\text{V}$ as can be seen in figure 16 the

E. STEP CHANGE IN INPUT VOLTAGE

Operating at steady state operating point corresponds to $V_{oref} = 30$ volts the input voltage is changed in a step wise fashion. At time $t=0.4$ ms the input voltage is increased for $V_s = 10$ V to $V_s = 15$ V. The transient response of the converter is depicted in Figure 17 the output voltage remains practically unaffected with no undershoot observed while the controller settles very quickly at the new steady state operating conditions.



(a) Output voltage (solid line) reference (dashed line)

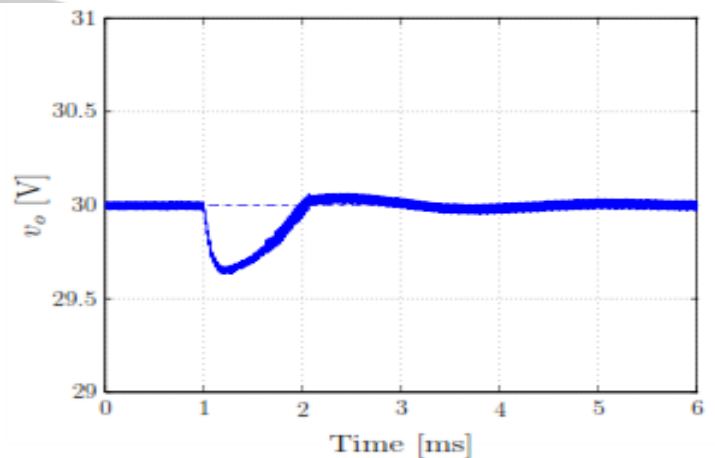


(b) Inductor current

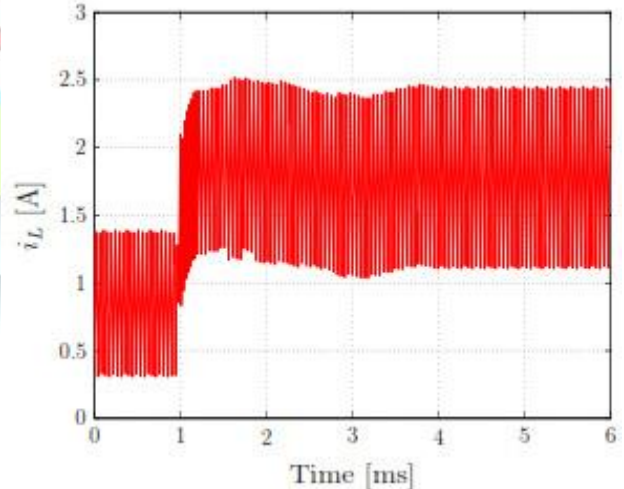
Figure 17 simulation result for step down change in Input voltage reference

F. LOAD STEP CHANGE

The last case examined is that of a drop in the load resistance as can be seen in figure 18 a step down change in the load from $R=73\Omega$ to $R=36.5\Omega$ occurs at $t=1$ ms (the input voltage is $V_s=15$ V and the output voltage reference is $V_{0,ref}=30$ V). The kalman filter adjusts the output voltage reference to its new value so as to avoid any steady state tracking error. This can be observed in fig 18 (a) after it has settled at the new operating point the output voltage accurately follows its reference.



(a) Output voltage (solid line) reference (dashed line)



(b) Inductor current

Figure 18 simulation result for step down change in load



G DISCUSSION

For the above simulated forms its clear that current mode and voltage mode controller formulated in the frame work of model predictive control (MPC) have been proposed. The discret time model of the converter used by both current mode and voltage controller is designed in such that it accurately predicts the plant behavior both when operating in continuous (CCM) as well as in Discontinuous conduction mode(DCM) as a resul the formulated contrller is applicable to the whole operating regime rather than just to a particular operaing point. For the current mode controller two different MPC approaches based on enumeration have been introduced. The implementaion of MPC as acurrent controller (rather than voltage controller) enabels the use of relatively short prediction horizon since the current exhibits the minimum phase behavior with respect to the control input . Therefore the required computational power is significantly reduced.The outer loop is loop is augumened by kalman filter suitable for all operating modes. This state estimation scheme is designed so as to cope with all possible disturbances and uncertainites, which might arise from real world non idealites. To this end the controller aims at rejecting all disturbances including load and input voltage variations.The performance of the proposed methods are compared via simulations. Both MPC approaches yeild a similar favorable. A load estimation scheme namely discrete tiem switched kalman filter is implemented to adress time varying unknown loads and to ensure robustness to parameter variations thaks to its integrating action it provides offset free tracking of the output voltage simulation results demonstrates the potential advantages of the proposed methodologies.

VII CONCLUSION

The proposed scheme carry several benefits such as fast dynamics achieved by MPC combined with its inherent properites are some of its key beneficial charctersitscs. Furthermore the fact that the control objectives are expressed in objective function in straight forward manner the design process is simple and laborious tuning is avoided is implemented. The variation of load is also predicted using kalman filter to drive better control signal, both the voltage and current control

methodology incorporated with MPC and Kalman filter is simulated in simulator in order to verify the versatility and effectiveness of the proposed technique and the proposed thechnique shows good response even for the variation in load.

VIII REFERENCES

- [1] J. Alvarez-Ramírez, I. Cervantes, G. Espinosa-Pérez, P. Maya, and A. Morales. A stable design of PI control for dc-dc converters with an RHS zero. *IEEE Trans. Circuits Syst. I*, 48(1):103–106, Jan. 2001.
- [2] A. G. Beccuti, S. Mariéthoz, S. Cliquennois, S. Wang, and M. Morari. Explicit model predictive control of dc-dc switched-mode power supplies with extended Kalman filtering. *IEEE Trans. Ind. Electron.*, 56(6):1864–1874, Jun. 2009.
- [3] A. G. Beccuti, G. Papafotiou, R. Frasca, and M. Morari. Explicit hybrid model predictive control of the dc-dc boost converter. In *Proc. IEEE Power Electron. Spec. Conf.*, pages 2503–2509, Orlando, FL, Jun. 2007.
- [4] Christo Ananth, S. Esakki Rajavel, S. Allwin Devaraj, P. Kannan. "Electronic Devices." (2014): 300.
- [5] Y. T. Chang and Y. S. Lai. Online parameter tuning technique for predictive current-mode control operating in boundary conduction mode. *IEEE Trans. Ind. Electron.*, 56(8):3214–3221, Aug. 2009.
- [6] J. Chen, A. Prodić, R. W. Erickson, and D. Maksimović. Predictive digital current programmed control. *IEEE Trans. Power Electron.*, 18(1):411–419, Jan. 2003.
- [7] Z. Chen, W. Gao, J. Hu, and X. Ye. Closed-loop analysis and cascade control of a nonminimum phase boost converter. *IEEE Trans. Power Electron.*, 26(4):1237–1252, Apr. 2011.
- [8] R. W. Erickson, S. Cuk, and R. D. Middlebrook. Large-signal modelling and analysis of switching regulators. In *Proc. IEEE Power Electron. Spec. Conf.*, pages 240–250, Cambridge, MA, Jun. 1982.
- [9] T. Geyer, G. Papafotiou, R. Frasca, and M. Morari. Constrained optimal control of the step-down dc-dc converter. *IEEE Trans. Power Electron.*, 23(5):2454–2464,



Sep. 2008.

[10] T. Geyer, G. Papafotiou, and M. Morari. Hybrid model predictive control of the step-down dc-dc converter. *IEEE Trans. Control Syst. Technol.*, 16(6):1112–1124, Nov. 2008.

[11] T. Geyer, G. Papafotiou, and M. Morari. Hybrid model predictive control of the step-down dc-dc converter. *IEEE Trans. Control Syst. Technol.*, 16(6):1112–1124, Nov. 2008.

[12] T. Gupta, R. R. Boudreaux, R. M. Nelms, and J. Y. Hung. Implementation of a fuzzy controller for dc-dc converters using an inexpensive 8-b microcontroller. *IEEE Trans. Ind. Electron.*, 44(5):661–669, Oct. 1997.

[13] M. K. Kazimierczuk and A. Massarini. Feedforward control dynamic of dc/dc PWM boost converter. *IEEE Trans. Circuits Syst. I*, 44(2):143–149, Feb. 1997.

[14] M. K. Kazimierczuk and L. A. Starman. Dynamic performance of PWM dc/dc boost converter with input voltage feedforward control. *IEEE Trans. Circuits Syst. I*, 46(12):1473–1481, Dec. 1999.

[15] A. Kugi and K. Schlacher. Nonlinear H_∞ controller design for a dc-to-dc power converter. *IEEE Trans. Control Syst. Technol.*, 7(2):230–237, Mar. 1999.

[16] F. H. F. Leung, P. K. S. Tam, and C. K. Li. The control of switching dc-dc converters—A general LQR problem. *IEEE Trans. Ind. Electron.*, 38(1):65–71, Feb. 1991.

[17] F. H. F. Leung, P. K. S. Tam, and C. K. Li. An improved LQR-based controller for switching dc-dc converters. *IEEE Trans. Ind. Electron.*, 40(5):521–528, Oct. 1993.

[18] P. Mattavelli, L. Rossetto, and G. Spiazzi. Small-signal analysis of dc-dc converters with sliding mode control. *IEEE Trans. Power Electron.*, 12(1):96–102, Jan. 1997.

[19] P. Mattavelli, L. Rossetto, G. Spiazzi, and P. Tenti. General-purpose fuzzy controller for dc-dc converters. *IEEE Trans. Power Electron.*, 12(1):79–86, Jan. 1997.

[20] Y. Qiu, H. Liu, and X. Chen. Digital average current-mode control of PWM dc-dc converters without current sensors. *IEEE Trans. Ind. Electron.*, 57(5):1670–1677, May 2010.

[21] I. Takahashi and T. Noguchi. A new quick-response and high-efficiency control strategy of an induction motor. *IEEE Trans. Ind. Appl.*, IA-22(5):820–827, Sep. 1986.

[22] J. Xu, G. Zhou, and M. He. Improved digital peak voltage predictive control for switching dc-dc converters. *IEEE Trans. Ind. Electron.*, 56(8):3222–3229, Aug. 2009.